Zoology 115 (2012) 47–57

Contents lists available at SciVerse ScienceDirect

Zoology

journal homepage: www.elsevier.de/zool

Prey handling using whole-body fluid dynamics in batoids

Cheryl D. Wilga[a,*], Anabela Maia[a], Sandra Nauwelaerts[b], George V. Lauder[c]

[a] Department of Biological Sciences, University of Rhode Island, 120 Flagg Road, Kingston, RI 02881, USA
[b] Department of Biology, Antwerp University, Universiteitsplein 1, B-2610 Antwerp – Wilrijk, Belgium
[c] Museum of Comparative Zoology, Harvard University, 26 Oxford Street, Cambridge, MA 02138, USA

ARTICLE INFO

Article history:
Received 22 April 2011
Received in revised form 10 August 2011
Accepted 14 September 2011

Keywords:
Benthic species
Functional morphology
Prey capture kinematics
Leucoraja erinacea
Urobatis halleri

ABSTRACT

Fluid flow generated by body movements is a foraging tactic that has been exploited by many benthic species. In this study, the kinematics and hydrodynamics of prey handling behavior in little skates, *Leucoraja erinacea*, and round stingrays, *Urobatis halleri*, are compared using kinematics and particle image velocimetry. Both species use the body to form a tent to constrain the prey with the pectoral fin edges pressed against the substrate. Stingrays then elevate the head, which increases the volume between the body and the substrate to generate suction, while maintaining pectoral fin contact with the substrate. Meanwhile, the tip of the rostrum is curled upwards to create an opening where fluid is drawn under the body, functionally analogous to suction-feeding fishes. Skates also rotate the rostrum upwards although with the open rostral sides and the smaller fin area weaker fluid flow is generated. However, skates also use a rostral strike behavior in which the rostrum is rapidly rotated downwards pushing fluid towards the substrate to potentially stun or uncover prey. Thus, both species use the anterior portion of the body to direct fluid flow to handle prey albeit in different ways, which may be explained by differences in morphology. Rostral stiffness and pectoral fin insertion onto the rostrum differ between skates and rays and this corresponds to behavioral differences in prey handling resulting in distinct fluid flow patterns. The flexible muscular rostrum and greater fin area of stingrays allow more extensive use of suction to handle prey while the stiff cartilaginous rostrum of skates lacking extensive fin insertion is used as a paddle to strike prey as well as to clear away sand cover.

1. Introduction

There has been great progress in understanding the fluid dynamics of feeding in fishes. Most of this progress is due to new techniques in visualizing and quantifying flow inside the oral cavities of suction-feeding fishes as well as the external environment around the head during prey capture (Ferry-Graham and Lauder, 2001; Ferry-Graham et al., 2003; Higham et al., 2005, 2006a,b; Nauwelaerts et al., 2007, 2008; Van Wassenbergh and Aerts, 2009). However, fluid dynamics studies of prey handling in fishes are lacking, likely due to the difficulty of tracking the movements of typically fast-moving predatory fish and prey organisms in the three-dimensional aquatic environment. Benthic predator–prey systems, which generally are more two-dimensional, may provide a suitable model for studying the fluid dynamics of prey handling.

Many fish species manipulate the surrounding water during prey handling using body parts other than the mouth. Manta (*Mobula*, *Manta*) and cownose rays (*Rhinopterus*) use cephalic lobes, which are modified anterior extensions of the pectoral fins, to direct flow and prey into the mouth when swimming in the water column, while cownose rays use the lobes to create feeding depressions in the substrate and to surround prey to increase the effectiveness of oral suction using wall effects (Notarbartolo-Di-Sciara and Hillyer, 1989; Sasko et al., 2006; Fisher et al., 2011). Some sharks, like hammerheads (*Sphyrna*), and guitarfish (*Rhinobatos*) will use the rostrum to pin prey against the substrate before maneuvering the mouth into position for capture (Strong et al., 1990; Wilga and Motta, 1998). Skates and rays use the body and pectoral fins to toss sediment onto the body to increase crypsis for ambush hunting or predator avoidance (Cook, 1971). Skates and rays also blow water from the mouth and gill slits to fluidize sand to uncover buried prey or remove attached prey from the substrate (Bigelow and Schroeder, 1953; Babel, 1967; Howard et al., 1977; Gregory et al., 1979; Schwartz, 1989; VanBlaricom, 1976; Sasko et al., 2006; Dean and Motta, 2004). Lesser electric rays, *Narcine brasiliensis*, protrude the jaws into the sand to extricate buried prey (Dean and Motta, 2004). We have observed skates, *Leucoraja erinacea*, and stingrays, *Urobatis halleri*, using the pectoral fins and rostrum to dislodge buried or attached prey in tanks with and without a sandy substrate. *Raja erinacea* will use the pectoral fins, rostrum and jaws to excavate and destroy an agar chamber containing natural live prey items (Wright and Wilga, unpublished data).

* Corresponding author. Fax: +1 401 874 4256.
E-mail address: cwilga@uri.edu (C.D. Wilga).

0944-2006/$ – see front matter © 2011 Elsevier GmbH. All rights reserved.
doi:10.1016/j.zool.2011.09.002

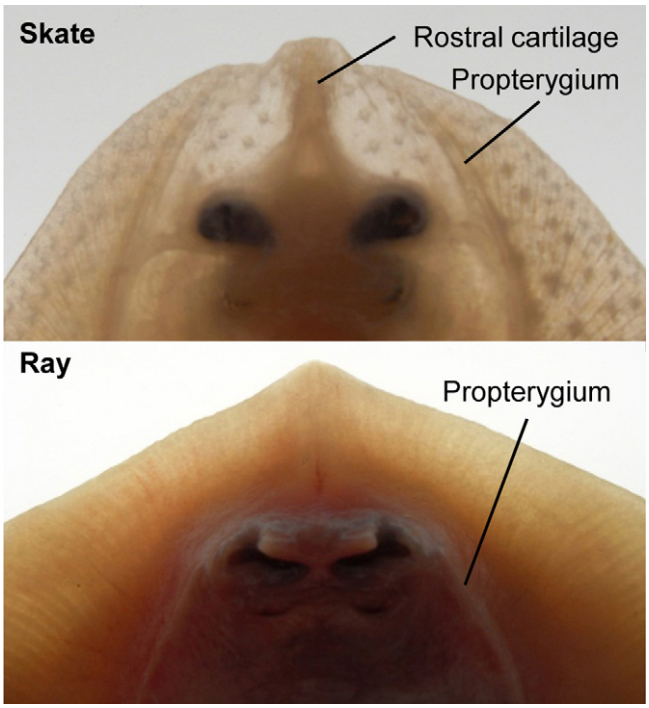

Fig. 1. Ventral view of a representative little skate (top) and round stingray (bottom) from the mouth to the rostral tip illuminated from beneath. Note the rostral cartilage in the skate, lacking in rays. Note also that the propterygium extends to the anterior margin of the pectoral fin in the skate and ends at the nasal capsule in the ray.

Taxonomic differences in rostral morphology between the sister groups Rajiformes (skates and guitarfishes) and Myliobatiformes (crown group including stingrays, and butterfly, eagle, cownose and devil rays) (Compagno, 1977; Nelson, 1994) should affect the mechanism of benthic prey handling using the anterior body (Fig. 1). In rajiform species, a robust rostral cartilage is present that stiffens the rostrum (Garman, 1913; Compagno, 1977; Shirai, 1996; McEachran et al., 1996). The webbing of the pectoral fins does not extend much past the eyes anteriorly, leaving skates with a distinct triangular rostrum separating the two sides anteriorly (Garman, 1913; Compagno, 1977; McEachran et al., 1996; Shirai, 1996). Skates essentially have a stiff paddle-like rostrum that would require powerful control by rostral elevator and depressor muscles (Marion, 1905; Garman, 1913; Wilga and Motta, 1998). In contrast, a rostral cartilage is absent in myliobatiform rays (Garman, 1913; Compagno, 1977; McEachran et al., 1996; Shirai, 1996; Schaefer and Summers, 2005). The webbing of the pectoral fins extends anterior to the cranium where the two sides merge; thus, myliobatiform rays have a flexible rostrum comprised of pectoral fin radials and ceratotrichia controlled by numerous muscle bundles.

In the present study, prey handling behavior using the body, rather than the mouth, in little skates, *L. erinacea* (Rajiformes), and round stingrays, *U. halleri* (Myliobatiformes), is compared using kinematics and fluid dynamics. Rostral, head and pectoral fin movements and the resulting fluid flow are analyzed using kinematics and digital particle image velocimetry. We hypothesize that the difference in stiffness of the rostrum and extent of pectoral fin attachment onto the head between the species will result in behavioral and flow differences. The more flexible rostrum and greater fin area of *U. halleri* will allow more extensive use of body suction to entrap and draw prey under the body, while the stiffer rostrum and smaller fin area of *L. erinacea* will be used as a paddle to push water and pin prey against the substrate.

2. Methods

2.1. Animals

Four little skates, *L. erinacea* (disc width (DW) 30–41 cm), were obtained by trawl from Narragansett Bay, RI, USA. Four round stingrays, *U. halleri* (DW 8–11 cm), were purchased from fish wholesalers (SeaDwelling Creatures, Los Angeles, CA, USA). Species were housed separately, skates in 1135 l and rays in 643 l circular tanks at $16 \pm 2\,^{\circ}C$ and $22 \pm 2\,^{\circ}C$, respectively, and maintained on a diet of squid (*Loligo* sp.) and fish (*Menidia menidia*). Food was withheld from individuals for three days prior to the experiment.

2.2. Digital particle image velocimetry

Each individual fish was acclimated to the experimental tank prior to each experiment. Pieces of squid (1.5 cm × 3 cm for skates and 0.5 cm × 1.0 cm for rays) were impaled on an L-shaped black wire and held pressed against the substrate to simulate attached prey. The density of sand interferes with neutrally buoyant particle movement and calculation of fluid flow; therefore no sand was used on the glass bottom tanks used for the experiments. Firmly holding the prey against a smooth substrate stimulates similar movements of the head and pectoral fins as those we observed with fish on sand.

The area of the fluid flow around the feeding fish was visualized and quantified using digital particle image velocimetry (DPIV). Water in the experimental tank was seeded with silver-coated, near neutrally buoyant, reflective particles of 12–14 μm diameter (Potter Ind., Valley Forge, PA, USA) at a density of 6.6 mg l^{-1}. A light beam from a continuous or pulsed argon-ion laser was focused into a vertical sheet 1–2 mm thick and 15 cm wide from below to illuminate the plane around the prey and predator. A high-speed, high-resolution (1024 × 1280 pixels) video camera (Photron USA, Inc., San Diego, CA, USA) was placed perpendicular to the laser sheet to record a lateral view of the fish and particle movement at 500 frames s^{-1} for the smaller rays and 250 frames s^{-1} for the larger skates. The fluid flow pattern around the body was recorded as the fish attempted to remove the squid from the wire.

Images were processed with DaVis 7.2 software (LaVision, Ypsilanti, MI, USA) using a sequential cross-correlation without pre-processing. An initial correlation window of 32 × 32 pixels was selected using multipass with window size decreasing to a final interrogation frame of 16 × 16 pixels with 50% overlap. Vector validation was performed, rejecting any vectors with a magnitude

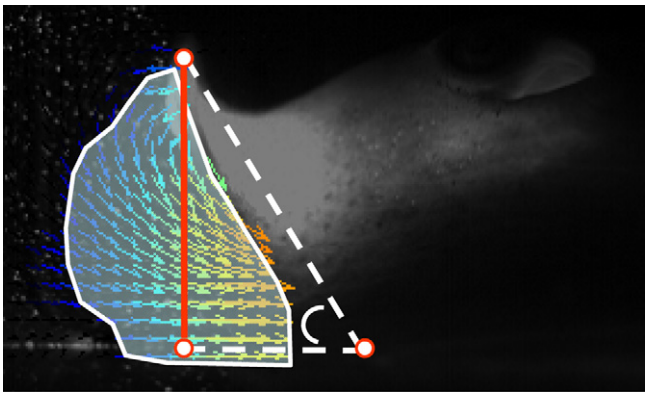

Fig. 2. Lateral view of a representative image of a ray feeding event at maximum rostral lift showing results of digital particle image velocimetry and kinematic measurements. White dots and dotted lines indicate rostral lift angle. Red line indicates rostral height. Area surrounded by the shaded white line indicates area of fluid flow moved.

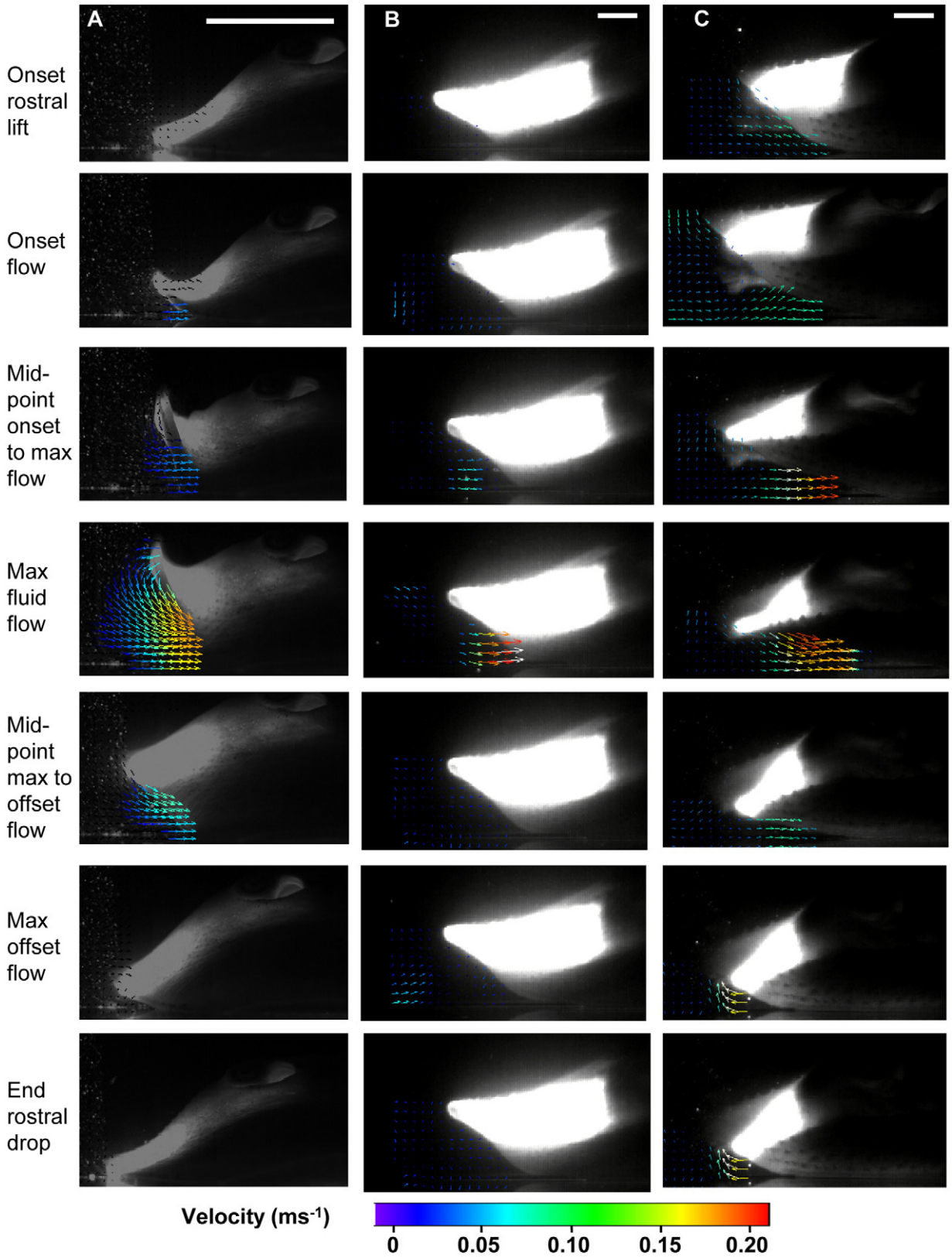

Fig. 3. Fluid dynamics results for skate and ray prey handling. Representative handling events illustrating rostral lift and drop with surrounding fluid flow for (A) stingray showing strong flow directed under the body due to rapid rostral lift, (B) skate showing strong flow under the body due to rapid rostral lift, and (C) skate showing strong flow directed under the body due to rapid rostral drop or rostral strike. Scale bar = 10 cm.

greater than two standard deviations from the mean. Vectors interpolated from surrounding vectors replaced rejected vectors. The resulting vector plots representing fluid flow were displayed using the corresponding video image for background and color-coded vectors indicating velocity. The area of significant flow was calculated as the area comprising all flow vectors moved by the fish with a velocity higher than the threshold velocity of 10% of maximum flow (after Muller and Osse, 1984; Day et al., 2005; Nauwelaerts et al., 2007). Procedures followed those used previously (Wilga and Lauder, 2002, 2004; Nauwelaerts et al., 2007, 2008).

2.3. Variables analyzed

Four prey handling sequences in which the mid-sagittal axis of the body was aligned within the laser sheet were analyzed from each of four individual *U. halleri* and *L. erinacea*. Each sequence was analyzed as a matrix of vectors from the onset of rostral lift until the rostrum was dropped. The time of onset, maximum and offset of significant flow was determined using the threshold value and vector matrices. Fluid velocity area was measured from velocity matrices exported from the frame of maximum fluid velocity for each sequence using ImageJ (NIH Image, Bethesda, MD, USA; Fig. 2). The maximum and mean fluid velocities of all the vectors in each area were calculated for each feeding event. The time at which the rostrum and head begin to elevate, maximum rostral and head lift and the end of rostral and head lift were determined. Time zero is the time of onset of rostral lift and the end of the sequence is the time when rostral drop ends for all behaviors. Rostral lift height from the substrate and rostral lift angle were calculated for each event in the frame of maximum rostral lift using ImageJ (Fig. 2). Rostral lift angle was calculated as the angle between the line from the tip of the rostrum to the point where the pectoral fin contacts the substrate and a line from the latter to the point directly below the tip of the rostrum on the substrate.

2.4. Statistics

The variables above were tested for significant differences among means by species and behavior (rostral lifts, rostral drops) using SAS v.9.2 (SAS Institute Inc., Cary, NC, USA). The data were tested for normality (Shapiro–Wilk *W* test) and homogenous variances. One-way ANOVAs were used to test for differences by behavior and species. Tukey tests were used as post hoc tests for ANOVA. When data could not be transformed to normality or homogenous variances, the Kruskal–Wallis one-way analysis of variance by ranks and Dunn's multiple comparison tests were used. Multiple stepwise linear regressions were used to test for relationships between fluid flow and kinematics.

3. Results

U. halleri and *L. erinacea* showed behavioral and hydrodynamic differences when attempting to take prey held fast to the bottom. *U. halleri* swam over the prey and pressed the pectoral fin edges against the substrate to constrain the prey. *U. halleri* then made a tent over the prey by rapidly raising the head away from the substrate while curling only the anteriormost edge of the pectoral fins upwards and away from the substrate to form an anterior opening. This rapid elevation of the head generated suction that draws a flow of fluid from the area in front of the ray through the opening formed by the upturned rostrum and the substrate and under the body. The lateral edges of the pectoral fins remained pressed against the substrate during this behavior (Figs. 3A and 4A). Flow continued to be drawn under the body as the rostrum started to drop due to continued elevation of the head and ended as the rostrum again contacted the substrate (Fig. 5). *L. erinacea* showed a similar tenting and suction behavior. However, the lateral sides of the rostrum were open to the environment as the rostrum was rotated upward, drawing fluid by suction broadly around the rostrum and under the body, while the pectoral fins remained pressed to the substrate (Figs. 3B and 4B). However, unlike *U. halleri*, the

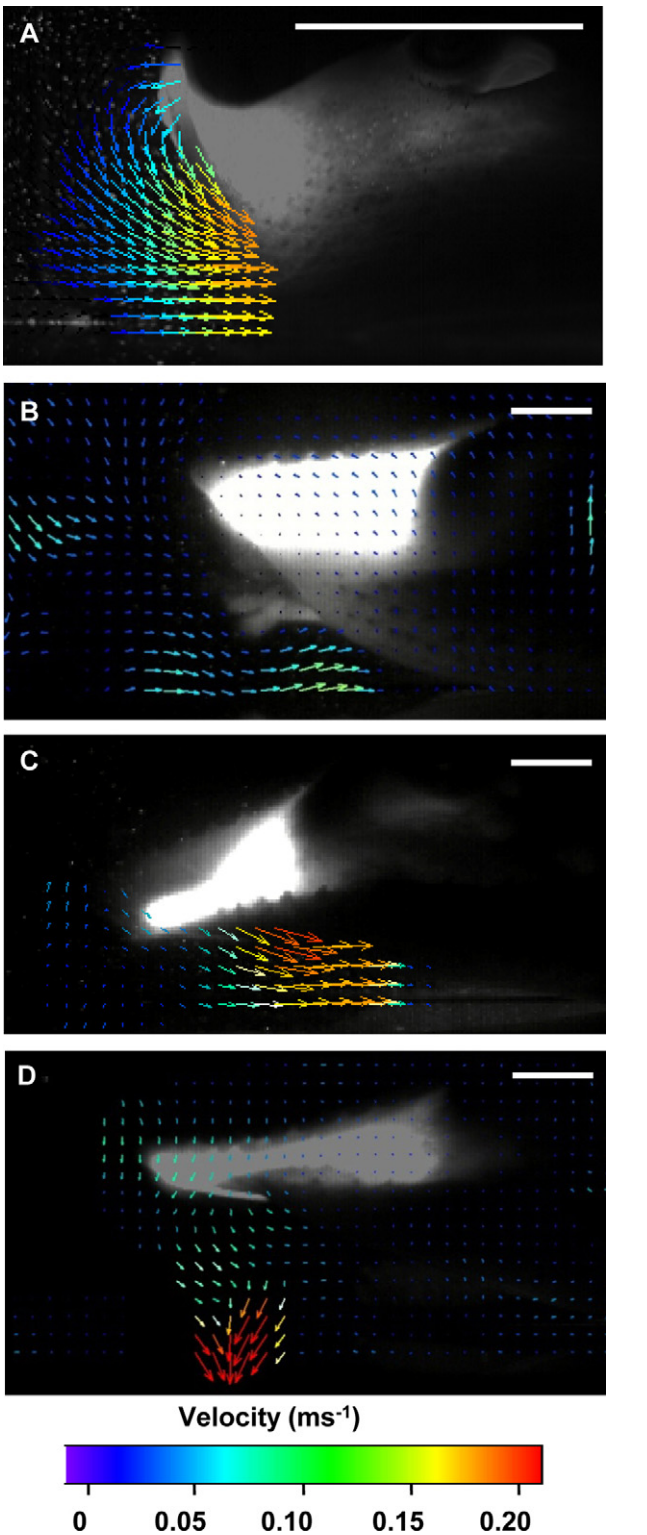

Fig. 4. Larger view of representative images illustrating the rostrum and surrounding fluid flow at maximum velocity for (A) stingray rostral lift with strong flow directed under the body, (B) skate rostral lift with weaker flow directed under the body, (C) skate rostral strike with strong flow directed under the body, and (D) skate rostral strike with strong flow pushed then released towards the substrate. Scale bar = 10 cm.

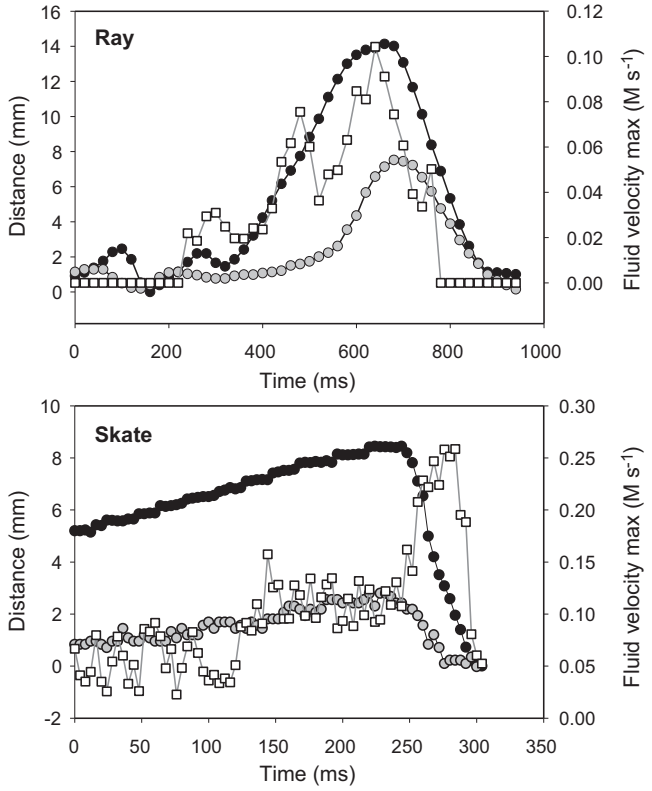

Fig. 5. Representative plots showing rostral and head kinematics and maximum fluid velocity during prey handling events in a stingray and a skate. ● rostrum; ◌ head; □ fluid velocity.

rostrum was rapidly rotated downwards after maximum rostral lift in *L. erinacea*, pushing fluid towards the substrate or under the body (Figs. 3C, 4C and D, and 5).

Fluid flow was analyzed during rostral lift and rostral drop/strike in all prey handling events for *L. erinacea* and *U. halleri* (Fig. 5). Fig. 6 represents individual and mean profiles of fluid velocity over a line extending from the mid-point of fluid flow at the body end (mouth end) through the mid-point of fluid flow at the level of the rostral tip into the environment until non-significant velocity. In both species, the posterior flap of the pectoral fins adjacent to the tail rose shortly after maximum rostral lift to allow fluid drawn under the body to exit; however, this was not always in view of the laser during experiments and thus was not analyzed.

Ray handling events were longer in duration than skate handling events (Table 2; Fig. 7). Temporal events were standardized by duration of the event from the onset of rostral lift (time 0) to the end of rostral drop to compare species. *U. halleri* achieved maximum rostral rotation height earlier than *L. erinacea* and had a longer duration of rostral drop (Table 2; Fig. 7). Suction flow towards the mouth position as the rostrum is raised was generated later in *U. halleri* than in *L. erinacea* (Table 2; Fig. 7). In addition, in *L. erinacea*, flow was also pushed towards the substrate as the rostrum was dropped in the rostral strike behavior (Tables 1 and 2; Figs. 6 and 7).

Magnitude variables were standardized by rostral lift height for comparisons between species and to other studies of oral suction feeding, since rostral lift is analogous to mouth opening. *U. halleri* had a smaller magnitude of rostral lift height but a larger rostral lift angle than *L. erinacea* (Tables 1 and 2). *U. halleri* generated faster standardized maximum fluid velocity during rostral lifts (suction flow) within the area of fluid moved than rostral lifts or drops in *L. erinacea*, as evidenced by the faster rate of rostral lift (Table 2). However, when comparing absolute values of maximum fluid velocity and standardized values of mean fluid velocity, they were greater during rostral lifts in *U. halleri* than during rostral lifts in *L. erinacea*, but similar to those during rostral drops in *L. erinacea*, where rostral lifts and drops were similar (Tables 1 and 2). Absolute mean flow was similar in all events for both species. Fluid flow area was greater during rostral lift events in both species than during rostral drop events in *L. erinacea*, and fluid flow duration was longer in *Urobatis* than in *Leucoraja* (Tables 1 and 2). The mean distance of significant fluid flow (10% of maximum value) was 1.5–2.3 rostral lift heights away from the mouth end and was similar in all events (Tables 1 and 2).

Multiple stepwise backward linear regressions were run to explore the relationship between fluid flow and kinematic events in *U. halleri* and *L. erinacea* (Tables 3 and 4, Figs. 8 and 9). Head variables had a greater effect on maximum and mean fluid velocity in *U. halleri* than rostral variables. In contrast, rostral variables contributed more to generating a larger area of accelerated fluid than head variables in *U. halleri*. In contrast to *U. halleri*, only one or two variables remained in most of the models for *L. erinacea*. All variables were eliminated from the model for maximum fluid velocity during rostral lifts. The larger the magnitude of rostral lift the larger the fluid area moved in rostral lift and drop events. Rostral drop appeared to curtail mean fluid velocity in rostral lifts, while a larger rostral lift contributed to a larger mean fluid velocity in rostral drops in *L. erinacea*. As expected, a greater velocity of rostral drop generated larger maximum fluid velocity in rostral drop events in *L. erinacea*.

4. Discussion

4.1. Fluid dynamics of prey handling

U. halleri and *L. erinacea* use different behavioral strategies to generate fluid flow to remove attached prey from the substrate. *U. halleri* raises the head to expand the volume between the head and substrate to generate a suction flow that is drawn under the body and through the opening created by curling up the flexible rostral tip from the substrate. *L. erinacea* shows a similar tenting and suction behavior as *U. halleri*. However, the smaller pectoral fin area leaves the sides of the rostrum open in *L. erinacea* and this results in weaker suction flow drawn under the body in *L. erinacea* which draws flow in from a broader area around the rostrum than *U. halleri*. *L. erinacea* also uses a rostral strike behavior during the head drop phase that pushes fluid towards the substrate or under the body, which is not observed in *U. halleri*. Rostral lifts and drops are often repeated several times and appear to function to stun or dislodge attached prey, but on sandy substrates could also fluidize sand for excavating prey.

Functionally, this prey handling behavior in *U. halleri* is similar to that of hydraulic suction feeding in fishes using the oral cavities (Lauder and Shaffer, 1993; Higham et al., 2006a,b; Nauwelaerts et al., 2008). The rapid curling of the flexible rostrum upwards from the substrate is analogous to the rapid mouth opening phase in suction-feeding fishes; both actions provide an opening for fluid to pass through. Elevation of the head vertically away from the substrate is analogous to depression of the hyoid ventrally in suction-feeding fishes; both provide the rapid expansion that generates the suction pressure within a cavity. The pectoral lateral edges remain pressed against the substrate occluding the lateral sides of the rostrum much like labial folds occlude the lateral sides of the mouth in suction-feeding fishes; both function to direct fluid flow anteriorly and increase fluid velocity by providing a smaller orifice. The head elevates independently from the muscular rostrum and extends the duration of fluid flow well past the time of maximum rostral lift (Figs. 5 and 7). Rostral and head movements of *U. halleri* generate roughly similar suction flow velocities as those generated by suction feeding in largemouth bass but considerably

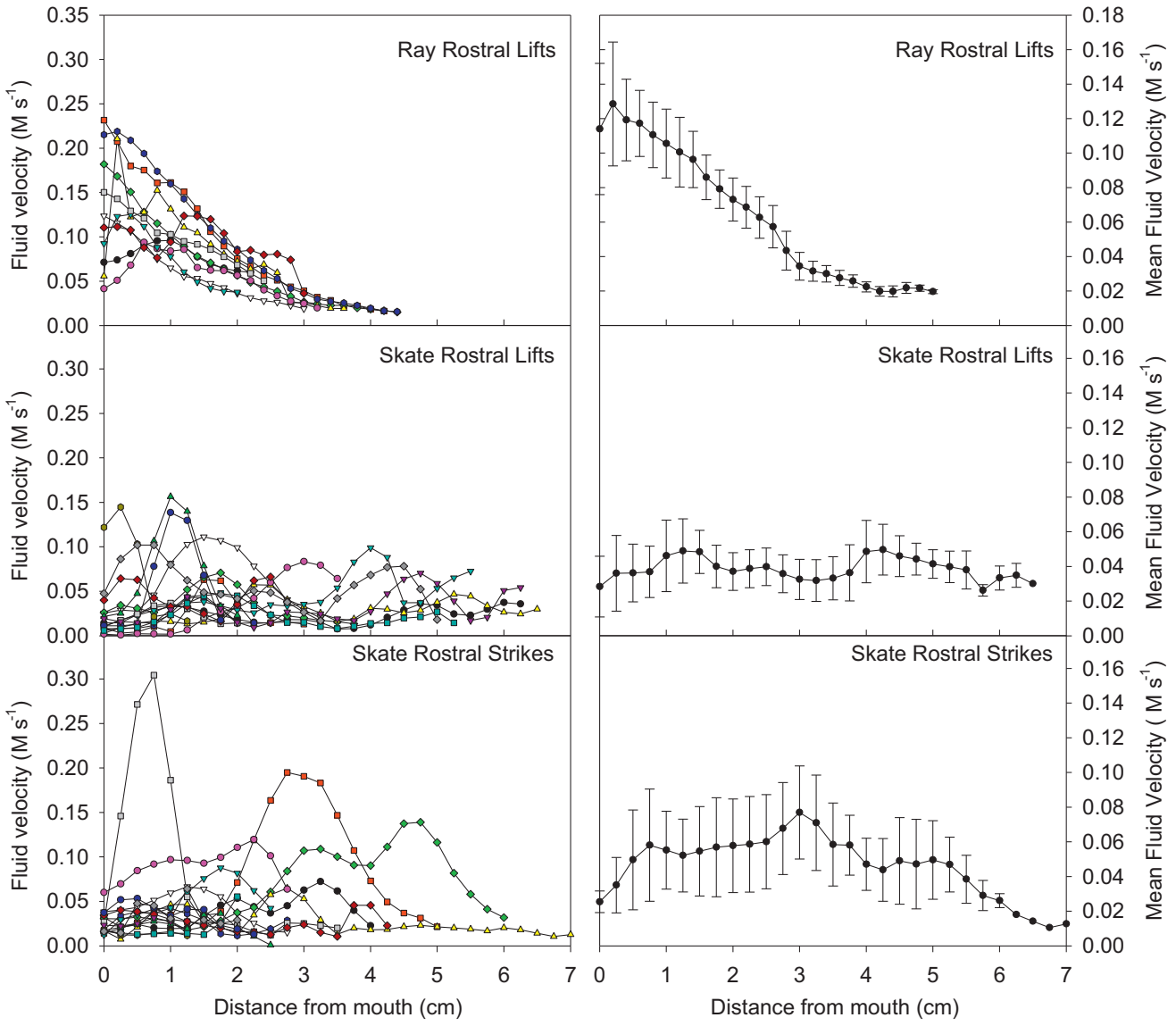

Fig. 6. Fluid velocity plots by distance from the mouth end of the body by individual (left) and means (right) in the image containing maximum fluid velocity for stingrays and skates. Different symbols and lines indicate different individuals. Mean plots also show standard error bars.

smaller than those of suction-feeding bluegill sunfish and white-spotted bamboo sharks (Higham et al., 2006b; Nauwelaerts et al., 2008) which are thought to be suction specialists (Wilga et al., 2011; Fig. 10).

In contrast, rostral movements in *L. erinacea* function more like a simple flat plate or fan rotated up and down through the water, providing drag-based fluid acceleration during each lift and drop phase (Webb and Blake, 1985). Rostral lifts generate suction flow directed towards the mouth end of the body that apparently functions to fluidize the substrate and/or move prey towards the mouth. Rostral drops push fluid towards the substrate or under the body, again moving the prey towards the mouth and/or fluidizing the substrate. We have observed skates using the rostrum and pectoral fins to excavate prey buried in sand; however, this behavior rapidly fluidizes the substrate making video recordings virtually useless (Wright and Wilga, unpublished data). The time of maximal fluid flow varies considerably during each rostral lift and drop phase indicating that skates have extensive control of rostral kinematics that may function to direct flow in variable directions depending on the handling event (Fig. 6). The large area of open space along the lateral edges of the rostrum in *L. erinacea* results in fluid escaping around the edges and weaker fluid flow generation compared to *U. halleri*. Other than fluid flow starting and peaking earlier in rostral lifts compared to rostral drops in *L. erinacea*, the kinematics and resulting flow are similar. Fluid flow generated by the rostrum of *L. erinacea*, whether lift or strike, appears to be weaker than suction flow generated by the oral cavity of largemouth bass, bluegill sunfish and white-spotted bamboo sharks (Fig. 10) (Higham et al., 2006b; Nauwelaerts et al., 2008).

The volume ingested by suction-feeding fishes such as bluegill, bass and bamboo sharks in the water column is generally confined to a radius of one mouth width distance from the mouth (Higham et al., 2006b; Nauwelaerts et al., 2007). However, the distance over which suction flow is effective can be extended when feeding near a substrate due to passive ground effects as shown by a doubling of the distance of effective suction flow in white-spotted bamboo sharks capturing prey on the substrate (Nauwelaerts et al., 2007; Van Wassenbergh and Aerts, 2009). *U. halleri* and *L. erinacea* use the same strategy to extend flow from 1.5 to 2.3 rostral height distances from the mouth end during prey handling. Thus, some benthic predators can take advantage of wall effects to extend the

Table 1
Stingray and skate prey handling variables (means ± S.E).

Variable	Ray lift	Skate lift	Skate strike
Fluid flow onset [ms]	144 ± 44	7 ± 5	94 ± 33
Fluid flow max [ms]	272 ± 74	55 ± 21	120 ± 30
Time to max fluid flow [ms]	128 ± 58	48 ± 21	25 ± 10
Fluid flow max velocity [m s^{-1}]	0.1549 ± 0.0275	0.0947 ± 0.0200	0.1329 ± 0.0413
Fluid flow max velocity [RH s^{-1}]	9.35 ± 1.83	4.51 ± 1.15	6.11 ± 2.18
Fluid flow mean velocity [m s^{-1}]	0.0497 ± 0.0064	0.0430 ± 0.0079	0.0485 ± 0.0108
Fluid flow mean velocity [RH s^{-1}]	3.08 ± 0.58	2.03 ± 0.45	2.20 ± 0.43
Fluid flow area max[a] [RH^2]	1.73 ± 0.65	0.70 ± 0.24	0.80 ± 0.23
Fluid flow distance[a] [RH]	2.27 ± 0.33	1.75 ± 0.43	1.55 ± 0.39
Fluid flow duration (on to end) [ms]	254 ± 74	76 ± 33	45 ± 13
Fluid flow offset [ms]	398 ± 89	83 ± 32	139 ± 33
Rostral lift rate[a] [RH/s]	7.75 ± 1.4	3.78 ± 2.10	3.78 ± 2.10
Rostral lift rate max[a] [%dur]	21 ± 10	27 ± 9	27 ± 9
Rostral lift max[a] [%dur]	34 ± 7	64 ± 8	64 ± 8
Rostral lift angle max [°]	56.26 ± 6.16	24.63 ± 4.32	24.63 ± 4.32
Rostral lift max [cm]	1.72 ± 0.22	2.19 ± 0.21	2.19 ± 0.21
Rostral drop duration[a] [%dur]	53 ± 6	29 ± 6	29 ± 7
Head lift onset [%dur]	12 ± 6	–	–
Head lift max [%dur]	59 ± 16	–	–
Head lift max (RH)	0.33 ± 0.10	–	–
Head lift max rate [%dur]	26 ± 10	–	–
Head lift max rate [RH s^{-1}]	7.76 ± 1.74	–	–
Head drop rate [%dur]	67 ± 12	–	–
Handling event duration [ms]	662 ± 140	136 ± 33	136 ± 33

RH, rostral lift height; %dur, percent duration from onset of rostral lift to end of rostral drop
[a] Variables standardized by rostral lift height.

reach of fluid flow in a variety of prey capture and prey handling behaviors despite slower flow.

Multiple stepwise regressions identified several variables that contribute to fluid flow velocity and area during prey handling behavior in *U. halleri* and *L. erinacea*. Head lift variables influence fluid flow velocity in *U. halleri*, suggesting that head lift is analogous to hyoid depression, which is primarily responsible for generating intraoral pressure in suction-feeding fishes (Lauder and Shaffer, 1993; Fig. 9). Note that individual prey handling events in *U. halleri* have more uniform fluid velocity profiles, typical of rapid suction events (Fig. 6). Rostral lift in conjunction with head lift contributes to a larger fluid flow area in *U. halleri*, which is analogous to mouth opening coupled with hyoid depression determining flow area in suction-feeding fishes (Lauder and Shaffer, 1993). In contrast, the magnitude of rostral lift, like a rotating paddle, primarily influences fluid velocity during lifts and drops in *L. erinacea* (Fig. 9). The lack of influential variables is likely a result of highly variable kinematics and fluid flow in lift and strike events in *L. erinacea* (see individual plots in Fig. 6). This may reflect the capacity to modulate rostral movements to match various prey handling situations.

4.2. Prey handling behaviors in batoids

Prey handling behaviors involving the rostrum and pectoral fins have been observed in many elasmobranchs, though primarily in batoids. Manta and cownose rays have extensions of the pectoral fins, the cephalic lobes, which are used in excavating the substrate, directing oral suction flow, and constraining prey escape (Schwartz, 1989; Notarbartolo-Di-Sciara and Hillyer, 1989; Sasko et al., 2006; Fisher et al., 2011). A similar behavior to that of *U. halleri* reported here was observed in *Rhinoptera bonasus* (Myliobatiformes) when excavating prey from the substrate (Sasko et al., 2006). A chamber around the mouth area is formed by the pectoral fins occluding the lateral sides of the posterior head region while the cephalic lobes

Table 2
Stingray and skate prey handling ANOVA results.

Variable	ANOVA	*F* or *H*-value	*P*-value	Differences
Fluid flow onset [ms]	KW Dunn	36.68	<0.001	RL > SS > SL
Fluid flow max [ms]	KW Dunn	31.169	<0.001	RL > SS > SL
Time to max fluid flow [ms]	KW Dunn	17.674	<0.001	RL > SL, SS
Fluid flow max velocity [m s^{-1}]	AN Tukey	4.365	0.018	RL, SS > SS, SL
Fluid flow max velocity [RH s^{-1}]	KW Dunn	17.241	<0.001	RL > SS, SL
Fluid flow mean velocity [m s^{-1}]	AN Tukey	2.222	0.329	
Fluid flow mean velocity [RH s^{-1}]	KW Dunn	10.873	0.004	RL, SS > SS, SL
Fluid flow area max[a] [RH^2]	KW Dunn	9.368	0.009	RL, SS > SS, SL
Fluid flow distance[a] [RH]	AN Tukey	6.026	0.049	
Fluid flow duration (on to end) [ms]	KW Dunn	28.801	<0.001	RL > SL, SS
Fluid flow offset [ms]	KW Dunn	34.516	<0.001	RL > SS, SL
Rostral lift rate[a] [RH s^{-1}]	KW Dunn	22.612	<0.001	RL > SS, SL
Rostral lift rate max[a] [%dur]	KW Dunn	1.722	0.423	
Rostral lift max[a] [%dur]	AN Tukey	21.849	<0.001	SS, SL > RL
Rostral lift angle max [°]	AN Tukey	59.663	<0.001	RL > SS, SL
Rostral lift max [cm]	AN Tukey	7.030	0.002	SS, SL > RL
Rostral drop duration[a] [%dur]	KW Dunn	22.093	<0.001	RL > SS, SL
Handling event duration [ms]	KW Dunn	34.650	<0.001	RL > SS, SL

AN Tukey, one-way ANOVA with Tukey multiple comparisons test; KW Dunn, Kruskal-Wallis one-way ANOVA with Dunn's multiple comparisons test; RH, rostral lift height; RL, ray lift; SS, skate strike; SL, skate lift; %dur, percent duration from rostral lift to rostral drop.
[a] Variables standardized by rostral lift height.

Table 3
Results from multiple stepwise linear regressions using flow variables as the dependent variables and kinematic variables as independent variables during prey handling events in *Urobatis halleri*.

Model and variables	Coefficient	Standardized coefficient	R^2	*F*-value	*P*-value
Maximum fluid velocity [m s^{-1}]			0.756	6.826	0.004
Rostral lift velocity max [ms]	−0.000405	−0.653	0.00153	7.277	0.021
Head lift onset [ms]	0.000542	0.682	0.118	12.186	0.005
Head lift max [ms]	−0.000297	−0.840	0.196	21.022	<0.001
Head lift max [cm]	0.149	0.743	0.223	12.808	0.004
Head lift velocity max [cm ms^{-1}]	10.375	0.524	0.217	9.800	0.010
Mean fluid velocity [m s^{-1}]			0.733	11.926	<0.001
Head lift max [cm]	0.0330	0.704	0.336	21.140	<0.001
Head lift velocity max [cm ms^{-1}]	−2.837	−0.612	0.284	17.960	<0.001
Head drop velocity max [cm ms^{-1}]	0.756	0.357	0.113	5.522	0.035
Maximum fluid area [cm^2]			0.740	3.656	0.037
Rostral lift rate max [ms]	−6.383	−2.014	0.00185	13.995	0.005
Rostral lift max [ms]	2.543	0.828	0.00390	4.716	0.058
Rostral lift angle max [°]	20.500	0.896	0.00333	5.687	0.041
Rostral lift max [cm]	−670.180	−1.062	0.152	5.541	0.043
Rostral drop duration [ms]	−2.596	−1.497	0.011	15.248	0.004
Head lift rate max [cm ms^{-1}]	143,499.443	1.415	0.122	18.731	0.002
Head lift rate max [ms]	4.513	2.196	0.446	15.423	0.003

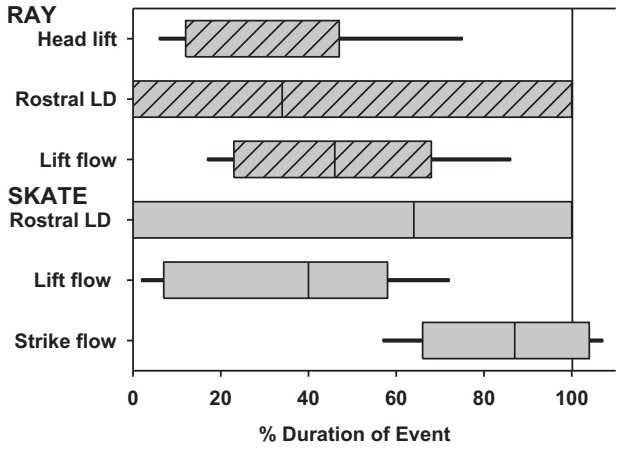

Fig. 7. Temporal variables for stingray and skate handling events standardized to duration of rostral lift to drop. Bars indicate mean onset and offset of the event. Vertical line between consecutive bars indicates the mean. Short black horizontal lines indicate standard error. LD, duration of lift, then drop with vertical line indicating time of maximum lift.

extend horizontally to occlude the lateral sides of the anterior head region as well as partly anteriorly (Sasko et al., 2006). A head bobbing behavior is observed in *R. bonasus* excavating in the wild that involves cyclical head elevation and depression to fluidize sediment (Sasko et al., 2006) that may be similar to the head lifting and dropping behavior that generates the fluid flow quantified here in *U. halleri*. Cephalic lobe depression during food capture in *R. bonasus* functions like rostral movement during prey handling quantified here in *U. halleri* to direct suction flow. Further studies of head and body kinematics, fluid dynamics, and intraoral pressure during prey excavation and prey handling behaviors in other elasmobranchs and predator–prey situations would reveal the prevalence of prey handling behaviors and how they correspond to phylogenetic history and ecology.

In contrast, rostral lifting in the lesser electric ray *N. brasiliensis* (Torpediniformes: Narcinidae) and the Atlantic guitarfish *Rhinobatos lentiginosus* (Rajiformes: Rhinobatidae) is comparable to that of *L. erinacea* (Wilga and Motta, 1998; Dean and Motta, 2004). In both of these species, the rostrum and head are lifted as one during food capture events while the pectoral fins remain pressed against the substrate although without the anterior enclosure formed by the rostral tip (Wilga and Motta, 1998; Dean and Motta, 2004). Although *N. brasiliensis* has electric organs, electric discharge appears to be used for predator defense rather than prey capture (Macesic and Kajiura, 2009). However, the Pacific electric ray *Torpedo californica* (Torpediniformes: Torpedinidae) uses the pectoral fins to surround fish prey while discharging the electric organ; these rays do not appear to use the rostrum to create suction to fluidize the substrate in the same manner as *U. halleri* (Bray and Hixon, 1978; Lowe et al., 1994).

Table 4
Results from multiple stepwise linear regressions using rostral lift and drop flow variables as the dependent variables and kinematic variables as independent variables during prey handling events in *Leucoraja erinacea*.

Model and variables	Coefficient	Standardized coefficient	R^2	*F*-value	*P*-value
Rostral lift					
Mean fluid velocity [m s^{-1}]			0.263	6.072	0.025
Rostral drop duration [ms]	0.000586	0.513	0.263	6.072	0.025
Maximum fluid area [cm^2]			0.416	5.702	0.014
Rostral lift angle max [°]	−13.132	−0.469	0.0215	5.888	0.027
Rostral lift max [cm]	297.353	0.522	0.201	7.288	0.016
Rostral drop					
Maximum fluid velocity [m s^{-1}]			0.906	4.609	0.047
Rostral drop velocity max [cm s^{-1}]	1.946	0.462	0.906	4.609	0.047
Mean fluid velocity [m s^{-1}]			0.00943	8.817	0.009
Rostral lift max [cm]	0.0280	0.584	0.00943	8.817	0.009
Maximum fluid area [cm^2]			0.246	5.542	0.031
Rostral lift max [cm]	290.921	0.496	0.246	5.542	0.031

Maximum fluid velocities [m s^{-1}]: all variables were eliminated from the model using the criterion settings.

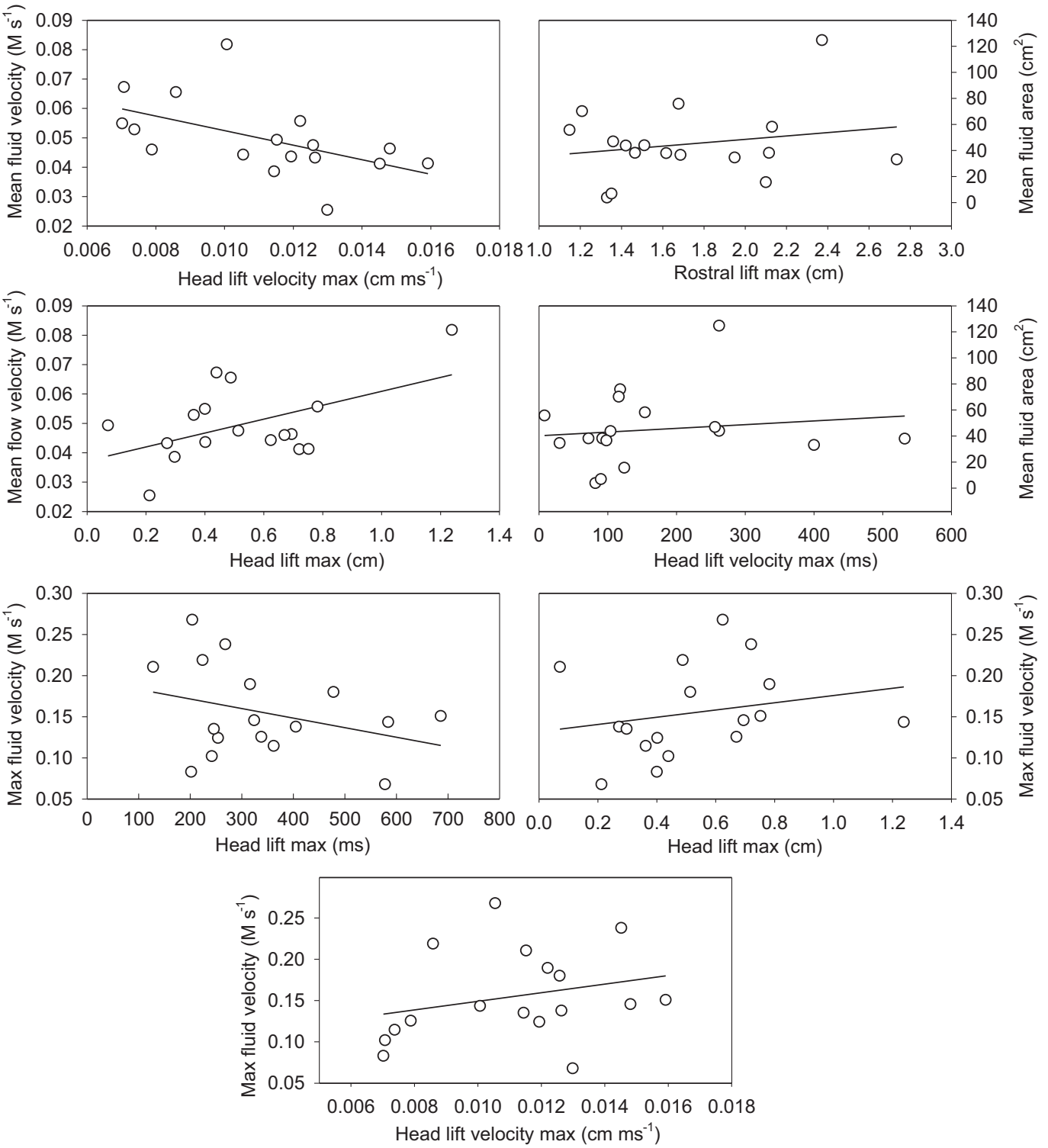

Fig. 8. Plots showing variables with an r^2 of at least 0.15 that contribute to fluid velocity and area in stingrays according to multiple backward stepwise regressions.

Some fluid movement may be due to contributions of suction or blowing by the mouth, which is obstructed from view by the fins; thus, any oral cavity contribution to fluid flow was not assessed here. However, the mouth is 1.4 rostral heights from the tip of the rostrum in *L. erinacea*, and 2.1 in *U. halleri*, and any oral fluid flow contribution beyond the range of the rostrum is likely to be negligible. Intraoral pressure during feeding in *L. erinacea* is relatively weak at a mean of −1.3 kPa (Wilga et al., 2007, 2011), but is sufficient to manipulate the small prey items within the oropharyngeal cavity that comprise the diet (Bigelow and Schroeder, 1953; Ebert and Bizarro, 2007). Pressure at the prey ingested by *N. brasiliensis* is much stronger (mean: −21.68 kPa) than that by *L. erinacea* (mean: −0.23 kPa) (Dean and Motta, 2004; Wilga et al., 2007). *N. brasiliensis* has relatively long tubular jaws with a small mouth opening that enhances suction while the relatively short jaws with open sides facilitate grasping in *L. erinacea* (Dean and Motta, 2004; Wilga et al., 2007, 2011). Intraoral suction in *L. erinacea* is likely insufficient to fluidize the substrate. In skate species that prey on benthic infauna,

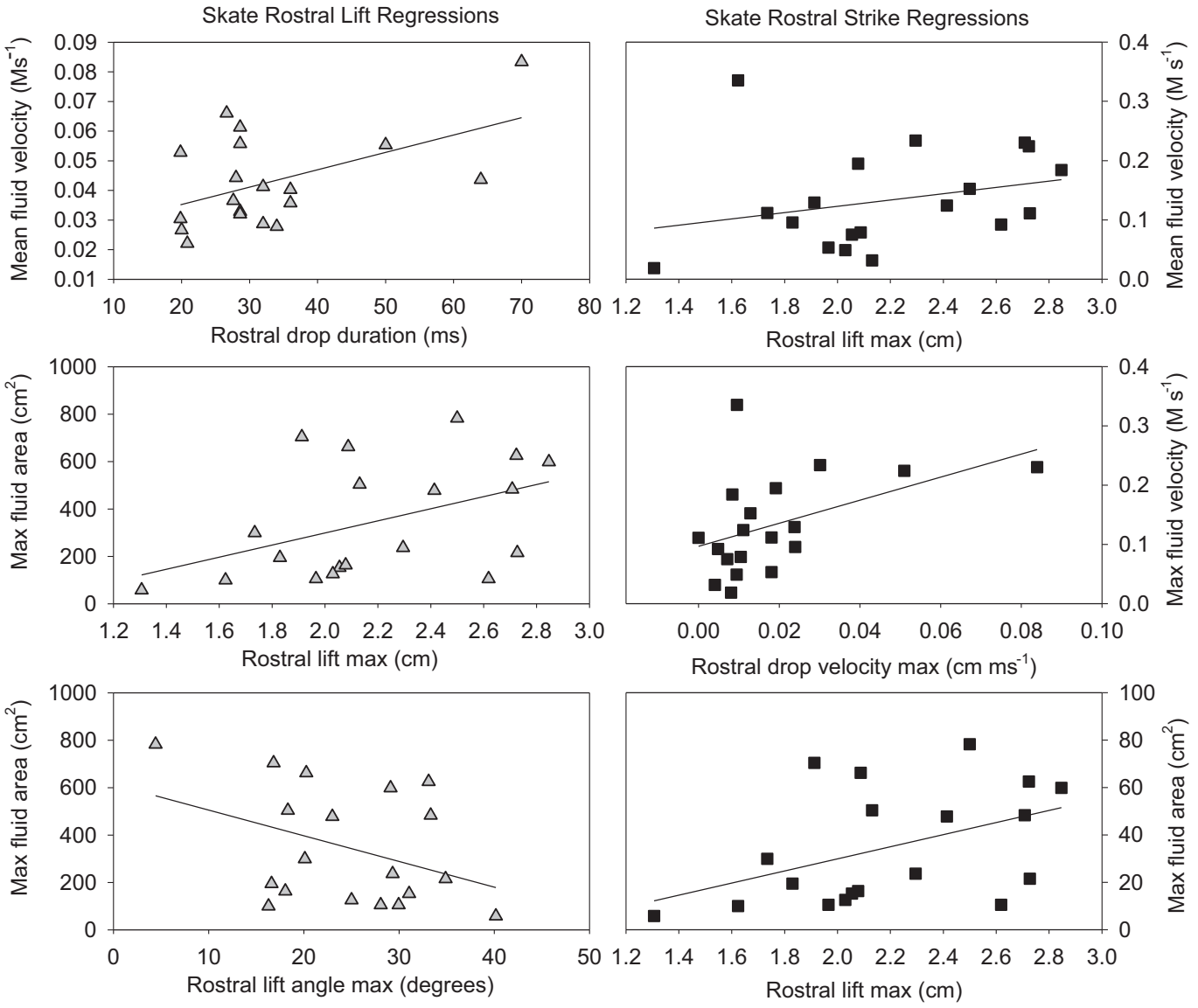

Fig. 9. Plots showing all variables that contribute to fluid velocity and area during rostral lifts (left side) and strikes (right side) in skates according to multiple backward stepwise regressions. Note that no variables were left in the model for maximum fluid velocity of skate rostral lifts.

rostral and pectoral fin behaviors that fluidize the substrate may compensate for the weak suction forces generated by the mouth.

The capacity to generate hydrodynamic forces by pectoral fin interactions with the substrate to burrow in the sand has been observed in many skate and ray species (Bigelow and Schroeder, 1953; Babel, 1967; Cook, 1971; VanBlaricom, 1976; Howard et al., 1977; Gregory et al., 1979; Schwartz, 1989). Burrowing behavior in *U. halleri* is the result of water expelled through the mouth with coordinated movement of the pectoral fins and is thought to provide crypsis but is also used for the dislodging of infaunal prey items (Babel, 1967). It appears that some benthic predators have an extensive repertoire of behaviors in which the flexible pectoral fins are used to interact with the substrate.

In summary, *L. erinacea* and *U. halleri* use the body to direct flow in different ways to accomplish similar prey handling tasks. *L. erinacea* uses simultaneous rostral and head movements due to the stiff cartilaginous connection between the rostrum and head to generate weak suction and moderate striking fluid flow. In contrast, *U. halleri* generates strong sustained suction flow using independent but coordinated movements of the rostrum and head. These differences may be due to the evolutionary divergence in rostrum

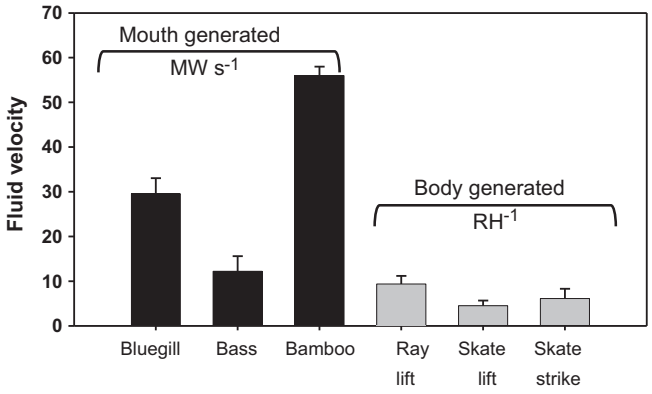

Fig. 10. Range of fluid velocity generated by the mouth and body during feeding in fishes. Fluid velocity is standardized to mouth (MW) in mouth-generated events and to rostral height (RH) in body-generated events. Lift = flow moved by rostral lifts; Strike = flow moved by rostral drops (bluegill and bass data after Higham et al., 2006a,b; bamboo data after Nauwelaerts et al., 2008).

(stiff and cartilaginous in skates; muscular and flexible in stingrays) and pectoral fin morphology (extensive in rays; limited in skates) leading to different prey handling behaviors since the two species feed on similar infauna (Garman, 1913; Bigelow and Schroeder, 1953; Babel, 1967; Compagno, 1977; Shirai, 1996; McEachran et al., 1996; Ebert and Bizarro, 2007). From an ecological perspective, stronger suction flow like that produced by *U. halleri* would be crucial to remove bivalves from the substrate, the preferential prey of this species in this size class (Babel, 1967). The extensive lateral line non-pored canals that surround the mouth of *U. halleri* would facilitate the detection of siphon currents emitted by these individuals (Jordan et al., 2009). In contrast, *L. erinacea* feeds mainly on amphipod crustaceans and polychaetes in the wild and for this type of prey stunning may be more effective (Ebert and Bizarro, 2007).

Acknowledgements

Thanks to Jack Szczepanski and Christopher Sanford for assisting in the skate experiments, to Lazaro Garcia and Dawn Simons for animal husbandry, and to two anonymous reviewers whose helpful comments improved the manuscript. This research was supported by NSF IBN-0344126 grant to C.D.W., a MCTES/FCT/SFRH/BD/36852/2007 grant to A.M., the University of Rhode Island, and Quaker Lane Bait and Tackle.

References

Babel, J.S., 1967. Reproduction, life history, and ecology of the round stingray, *Urolophus halleri* Cooper. Calif. Fish Game Bull. 137, 1–104.

Bigelow, H.B., Schroeder, W.C., 1953. Fishes of the Western North Atlantic. Part 2. Sawfishes, Guitarfishes, Skates and Rays, Chimaeroids. Sears Foundation for Marine Research, New Haven, CT.

Bray, R.N., Hixon, M.A., 1978. Night-shocker: predatory behavior of the Pacific electric ray (*Torpedo californica*). Science 200, 333–334.

Compagno, L.J.V., 1977. Phyletic relationships of living sharks and rays. Am. Zool. 17, 303–322.

Cook, D.O., 1971. Depressions in shallow marine sediment made by benthic fish. J. Sediment. Res. 41, 577–578.

Day, S.W., Higham, T.E., Cheer, A.Y., Wainwright, P.C., 2005. Spatial and temporal patterns of water flow generated by suction-feeding bluegill sunfish *Lepomis macrochirus* resolved by particle image velocimetry. J. Exp. Biol. 208, 2661–2671.

Dean, M.N., Motta, P.J., 2004. Feeding behavior and kinematics of the lesser electric ray, *Narcine brasiliensis* (Elasmobranchii: Batoidea). Zoology 107, 171–189.

Ebert, D.A., Bizarro, J.J., 2007. Standardized diet compositions and trophic levels of skates (Chondrichthyes: Rajiformes: Rajoidei). Environ. Biol. Fishes 80, 221–237.

Fisher, R.A., Call, G.C., Grubbs, R.D., 2011. Cownose ray (*Rhinoptera bonasus*) predation relative to bivalve ontogeny. J. Shellfish Res. 30, 187–196.

Ferry-Graham, L.A., Lauder, G.V., 2001. Aquatic prey capture in ray-finned fishes: a century of progress and new directions. J. Morphol. 248, 99–119.

Ferry-Graham, L.A., Wainwright, P.C., Lauder, G.V., 2003. Quantification of flow during suction feeding in bluegill. Zoology 106, 159–168.

Garman, S., 1913. The Plagiostoma (Sharks, Skates and Rays), vol. 36. Mem. Mus. Comp. Zool. at Harvard College, Cambridge.

Gregory, M.R., Ballance, P.F., Gibson, G.W., Ayling, A.M., 1979. On how some rays (Elasmobranchia) excavate feeding depressions by jetting water. J. Sediment. Petrol. 49, 1125–1130.

Higham, T.E., Day, S.W., Wainwright, P.C., 2005. Sucking while swimming: evaluating the effects of ram speed on suction generation in bluegill sunfish *Lepomis macrochirus* using digital particle image velocimetry. J. Exp. Biol. 208, 2653–2660.

Higham, T.E., Day, S.W., Wainwright, P.C., 2006a. The pressures of suction feeding: the relation between buccal pressure and induced speed in centrarchid fishes. J. Exp. Biol. 209, 3281–3287.

Higham, T.E., Day, S.W., Wainwright, P.C., 2006b. Multidimensional analysis of suction feeding performance in fishes: fluid speed, acceleration, strike accuracy and the ingested volume of water. J. Exp. Biol. 209, 2713–2725.

Howard, J.D., Mayou, T.V., Heard, R.W., 1977. Biogenic sedimentary structures formed by rays. J. Sediment. Petrol. 47, 339–346.

Jordan, L.K., Kajiura, A.M., Gordon, M.S., 2009. Functional consequences of structural differences in stingray sensory systems. Part I: Mechanosensory lateral line canals. J. Exp. Biol. 212, 3037–3043.

Lauder, G.V., Shaffer, H.B., 1993. Design of feeding systems in aquatic vertebrates: major patterns and their evolutionary implications. In: Hanken, J.H., Hall, B.K. (Eds.), The Skull: Functional and Evolutionary Mechanisms, vol. 3. University of Chicago Press, Chicago, pp. 113–149.

Lowe, C.G., Bray, R.N., Nelson, D.R., 1994. Feeding and associate behavior of the Pacific electric ray *Torpedo californica* in the field. Mar. Biol. 120, 161–169.

Macesic, L.J., Kajiura, S.M., 2009. Electric organ morphology and function in the lesser electric ray, *Narcine brasiliensis*. Zoology 112, 442–450.

Marion, G.E., 1905. Mandibular and pharyngeal muscles of *Acanthias* and *Raia*. Am. Nat. 39, 891–920.

McEachran, J.D., Dun, K.A., Miyake, M., 1996. Interrelationships of the batoid fishes (Chondrichthyes: Batoidea). In: Stiassny, M.L.J., Parenti, L.R., Johnson, G.D. (Eds.), Interrelationships of Fishes. Academic Press, San Diego, pp. 63–84.

Muller, M., Osse, J.W.M., 1984. Hydrodynamics of suction feeding in fish. Trans. Zool. Soc. Lond. 37, 51–135.

Nauwelaerts, S., Wilga, C.D., Sanford, C.P., Lauder, G.V., 2007. Hydrodynamics of prey capture in sharks: effects of substrate. J. R. Soc. Interface 4, 341–345.

Nauwelaerts, S., Wilga, C.D., Lauder, G.V., Sanford, C.P., 2008. Fluid dynamics of feeding behavior in white-spotted bamboo sharks. J. Exp. Biol. 211, 3095–3102.

Nelson, J.S., 1994. Fishes of the World, 3rd ed. Wiley, New York.

Notarbartolo-Di-Sciara, G., Hillyer, E.V., 1989. Mobulid rays off Eastern Venezuela. Copeia 1989, 607–614.

Sasko, D.E., Dean, M.N., Motta, P.J., Hueter, R.E., 2006. Prey capture behavior and kinematics of the Atlantic cownose ray, *Rhinoptera bonasus*. Zoology 109, 171–181.

Schwartz, F.J., 1989. Feeding behavior of the cownose ray, *Rhinoptera bonasus* (family Myliobatidae). ASB Bull. 36, 66.

Shirai, S., 1996. Phylogenetic interrelationships of neoselachians (Chondrichthyes: Euselachii). In: Stiassny, M.L.J., Parenti, L.R., Johnson, G.D. (Eds.), Interrelationships of Fishes. Academic Press, San Diego, pp. 9–34.

Strong Jr., W.R., Snelson Jr., F.F., Gruber, S.H., 1990. Hammerhead shark predation on stingrays: an observation of prey handling by *Sphyrna mokarran*. Copeia 1990, 836–940.

Schaefer, J.T., Summers, A.P., 2005. Batoid wing skeletal structure: novel morphologies, mechanical implications, and phylogenetic patterns. J. Morphol. 264, 298–313.

VanBlaricom, G.R., 1976. Preliminary observations on interactions between two bottom-feeding rays and a community of potential prey in a sublittoral sand habitat in Southern California. Pacific Northwest Technical Workshop, vol. WSG-WO 77-2, Washington Sea Grant, Astoria, OR, pp. 153–162.

Van Wassenbergh, S., Aerts, P., 2009. Aquatic suction feeding dynamics: insights from computational modeling. J. R. Soc. Interface 6, 149–158.

Webb, P.W., Blake, R.W., 1985. Swimming. In: Hildebrand, M., Bramble, D.M., Liem, K.F., Wake, D.B. (Eds.), Functional Vertebrate Morphology. Belknap Press, Cambridge, pp. 110–128.

Wilga, C.D., Lauder, G.V., 2002. Function of the heterocercal tail in sharks: quantitative wake dynamics during steady horizontal swimming and vertical maneuvering. J. Exp. Biol. 205, 2365–2374.

Wilga, C.D., Lauder, G.V., 2004. Hydrodynamic function of the shark's tail. Nature 430, 850.

Wilga, C.D., Motta, P.J., 1998. The feeding mechanism of the Atlantic guitarfish *Rhinobatos lentiginosus*: modulation of kinematic and motor activity. J. Exp. Biol. 201, 3167–3183.

Wilga, C.D., Motta, P.J., Sanford, C.P., 2007. Evolution and ecology of feeding in elasmobranchs. Integ. Comp. Biol. 47, 55–69.

Wilga, C.D., Duquette, A.A, Stoehrs, D.C., Allen, R.M., 2011. Functional ecology of feeding in elasmobranchs. Environ. Biol. Fishes, doi:10.1007/s10641-011-9781-7.